IEEE Access
Multidisciplinary | Rapid Review | Open Access Journal

Received August 14, 2020, accepted August 27, 2020, date of publication September 3, 2020, date of current version September 16, 2020.

Digital Object Identifier 10.1109/ACCESS.2020.3021094

Predefined-Time Polynomial-Function-Based Synchronization of Chaotic Systems via a Novel Sliding Mode Control

QIAOPING LI[1,2] AND CHAO YUE[1]

[1]School of Economics, Zhengzhou University of Aeronautics, Zhengzhou 450015, China
[2]School of Mathematics and Statistics, Xidian University, Xi'an 710071, China

Corresponding author: Qiaoping Li (liqiaoping1981@126.com)

This work was supported in part by the National Natural Science Foundation of China under Grant 11702201 and Grant 61877046, and in part by the Key Scientific Research Projects of Higher Education Institutions in Henan Province under Grant 19B110006 and Grant 20A110034.

ABSTRACT In the context of chaotic secure communication, this paper is concerned with the predefined-time polynomial-function-based synchronization of chaotic systems via sliding mode control. Firstly, a novel hybrid synchronization scheme among multiple chaotic systems based on polynomial function is defined. Subsequently, based on a new predefined-time stability criterion, a novel multi-power integral terminal sliding mode control algorithm is designed to realize the predefined-time polynomial-function-based synchronization. Finally, the secure communication simulation is presented to verify the feasibility and efficiency of the proposed synchronization scheme. The polynomial-function-based synchronization not only uses the addition and subtraction of vectors, but also uses the power multiplication of vectors, which makes the nonlinear structure of the composed drive system more complex, so that the communication scheme is more secure. Applying the sliding mode control algorithm designed in this work, the synchronization time can be preset off-line without estimation, moreover, the ratio between the formation time and the convergence time of sliding mode can also be distributed in advance, which is more flexible.

INDEX TERMS Polynomial-function-based synchronization, Predefined-time synchronization, Chaotic secure communication, multi-power integral terminal sliding mode control, and settling time function.

I. INTRODUCTION

With the development of internet and mobile communication, chaotic secure communication has attracted compelling attention over the last decades [1]–[7]. Chaotic synchronization is the foundation of chaotic secure communication, so further study on synchronization schemes and synchronization control technology can provide solid theoretical and technical support for the development of secure communication [8], [9].

On the one hand, security is an important indicator to measure the quality of the secure communication scheme. Increasing the complexity of the chaotic synchronization scheme is an important way to improve the security of the chaotic secure communication scheme. However, most synchronization methods involve only one driver system and one response system. In fact, if multiple chaotic systems are involved in the synchronization encryption scheme, the signal hiding method will be more flexible and more difficult to predict, which means the security of the communication scheme will be higher. To further improve the anti-attack capability of the synchronization technology in secure communication, R. Luo proposed a combination synchronization scheme consisting of two drive systems and a response system. The drive system in the above scheme can be regarded as a linear combination of two chaotic systems with the same dimension [10], [11]. Recently, Q. Li designed a novel synchronization scheme called ''modified function projective multi-lag generalized compound synchronization'', in which, not only the addition and subtraction, but also the multiplication of two chaotic systems are taken into consideration. This makes the signal hidden channels more abundant and the signal hidden methods more flexible. In addition, since the multiplication of chaotic systems is introduced in this synchronization scheme,

The associate editor coordinating the review of this manuscript and approving it for publication was Di He.

the diameter of the compound chaotic topological manifold become much longer, which means that more types of signals can be encrypted [12]. However, the above-mentioned compound synchronization only considers the multiplication of two matrices. If the synchronization scheme can be designed by using matrix polynomials, and the complexity of the synchronization scheme can be adjusted by changing the degree of the polynomial, then the attack resistance of the secure communication scheme will be improved effectively. This is the first motivation of this article.

On the other hand, synchronization time is another important indicator to measure the performance of the communication scheme since the encoded message cannot be recovered before the synchronisation is established. In the case of secure communication, fast synchronisation is required to avoid any loss of information at the initial stage [13]. Compared with asymptotic control, finite-time control has many advantages such as fast convergence, high accuracy and strong robustness. Therefore, finite-time synchronization has become more and more attractive in recent years [14]–[16]. The most important application of the finite-time convergence is the problem of differentiation, which allow the designer to be sure that the controller can use correct information after some time moment. That is why the upper bound of the settling time function for any initial conditions is crucial [17]. So it is necessary to introduce the fixed-time convergence, in which the settling time is uniformly bounded with respect to the initial conditions [18], [19]. In [20], the fixed-time convergence was applied to realize the fixed-time synchronization of complex networks with impulsive effects. In [21], the finite-time and fixed-time synchronization of discontinuous complex networks was designed based on a unified control framework. Nevertheless, the relationship between the upper bound of the settling time and the tuning gains in fixed-time convergence is not clear in general. Note that in the process of secure communication, the designer expects the encoded message can be recovered within any sufficiently short time given in advance, hence it is required to design a new synchronization control scheme with arbitrary synchronization time, applying which the synchronization time can be assigned in advance according to the designer's requirements. To achieve the objective, it is necessary to consider the concept of predefined-time convergence, for which an upper bound of the settling time function can be predefined off-line and is independent of initial conditions and any other design parameters [22]–[24]. As far as we know, there is few literature reporting the the predefined-time synchronization of chaotic systems.

In addition, sliding mode control (SMC) is an effective way to realize fast synchronization and is robust to parameter uncertainties and external disturbances [25], [26]. To weaken the chattering caused by the sign function in the traditional linear SMC, the integral terminal sliding mode control (ITSMC) was designed by introducing an integral compensation term into the function of terminal sliding mode surface [27], [28]. In [29], M. Hou proposed a model-free adaptive integral terminal sliding mode control method. It is a pity that the above ITSMCs are single-power and lack of flexibility. In [11], a novel multi-power ITSMC was designed to further suppress chattering and improve the convergence rate of sliding modes. However, the existing SMC schemes can not realize the predefined-time stability of sliding mode. So it is meaningful to design a predefined-time synchronization for multiple chaotic systems via SMC technology. This is anther motivation of our work.

Based on the above discussion, in this work, a novel synchronisation scheme is proposed to improve the security and accuracy of chaotic secure communication. The rest of this article is structured as follows: The preliminaries and problem description are statemented in Section II. Main theoretical results are presented in Section III. The simulation experiments of chaotic secure communication are carried out in Section IV to illustrate the validity and the advancement of the synchronization scheme. Finally, the conclusion and future work are reported in Section V and Section VI, respectively.

In contrast to the aforementioned results, the novelty and contributions that make this work more competitive can be summarized in three aspects.

- Firstly, by introducing the concept of polynomial function, a novel synchronisation scheme involving multiple chaotic systems is proposed, in which, the drive system is composed of multiple chaotic systems through mathematical operations such as addition, subtraction and power multiplication. Therefore, The topological structure of the compound drive system is more complex, and its chaotic path is more difficult to predict, which means better attack resistance as it applied in the secure communication. In addition, in this synchronisation scheme, the complexity of compound drive system can be adjusted by changing the degree of the polynomial, which is more flexible.
- Secondly, by introducing the predefined-time synchronization, the synchronization time can be pre-assigned off-line according to the task requirements and it can be arbitrarily short.
- Thirdly, the terminal sliding surface proposed in this work is multi-power, which can ensure the sliding mode is predefined-time stable. Moreover, the designer can determine the length of the sliding mode reaching time and the sliding mode convergence time by setting the time distribution weight according to the task requirement.

II. PRELIMINARIES AND PROBLEM DESCRIPTION

In this section, we introduce several precise definitions and important lemmas which are necessary for this work.

A. SYSTEM DESCRIPTION AND HYBRID SYNCHRONIZATION

The hybrid chaotic synchronization scheme designed in this work involves three basic drive systems and one response system which are described as below.

The first basic drive system

$$\begin{cases} \dot{x}_1(t) = F_1(x(t))\theta + f_1(x(t)) \\ \dot{x}_2(t) = F_2(x(t))\theta + f_2(x(t)) \\ \vdots \\ \dot{x}_n(t) = F_n(x(t))\theta + f_n(x(t)). \end{cases} \tag{1}$$

The second basic drive system

$$\begin{cases} \dot{y}_1(t) = G_1(y(t))\phi + g_1(y(t)) \\ \dot{y}_2(t) = G_2(y(t))\phi + g_2(y(t)) \\ \vdots \\ \dot{y}_n(t) = G_n(y(t))\phi + g_n(y(t)). \end{cases} \tag{2}$$

The third basic drive system

$$\begin{cases} \dot{z}_1(t) = H_1(z(t))\eta + h_1(z(t)) \\ \dot{z}_2(t) = H_2(z(t))\eta + h_2(z(t)) \\ \vdots \\ \dot{z}_n(t) = H_n(z(t))\eta + h_n(z(t)). \end{cases} \tag{3}$$

The response system

$$\begin{cases} \dot{w}_1(t) = R_1(w(t))\psi + r_1(w(t)) + u_1(t) \\ \dot{w}_2(t) = R_2(w(t))\psi + r_2(w(t)) + u_2(t) \\ \vdots \\ \dot{w}_n(t) = R_n(w(t))\psi + r_n(w(t)) + u_n(t), \end{cases} \tag{4}$$

where $x = [x_1, x_2, \cdots, x_n]^T$, $y = [y_1, y_2, \cdots, y_n]^T$ and $z = [z_1, z_2, \cdots, z_n]^T \in R^n$ denote the state vectors for the basic drive systems, $w = [w_1, w_2, \cdots, w_n]^T \in R^n$ represents the state vector of the response system. $f_i(x(t))$, $g_i(y(t))$, $h_i(z(t))$, and $r_i(w(t))$ are continuous nonlinear functions. $F_i(x(t))$, $G_i(y(t))$, $H_i(z(t))$ and $R_i(w(t))$ denote the ith rows of the continuous linear function matrices $F(x(t))$, $G(y(t))$, $H(z(t))$ and $R(w(t))$, respectively. $\theta = [\theta_1, \theta_2, \cdots, \theta_n]^T$, $\phi = [\phi_1, \phi_2, \cdots, \phi_n]^T$, $\eta = [\eta_1, \eta_2, \cdots, \eta_n]^T$ and $\psi = [\psi_1, \psi_2, \cdots, \psi_n]^T$ are system parameter vectors, $u = [u_1, u_2, \cdots, u_n]^T$ is the control input.

Definition 1: For vector $q = [q_1, q_2, \cdots, q_n]^T \in R^n$, a novel power multiplier is defined as below

$$q^{<l>} = [q_1^l, q_2^l, \cdots, q_n^l]^T, \tag{5}$$

where $l \in Z^+$ refers to the power. Based on (5), a novel polynomial about the vector q is defined as

$$P_N(q) = \sum_{l=1}^{N} A_l q^{<l>}, \tag{6}$$

where $N \in Z^+$ stands for the degree of the polynomial and $A_l = diag\{a_{l,1}, \cdots, a_{l,n}\}$ represents the coefficient matrix, $l = 1, 2, \cdots, N$.

Combining the vector polynomial (6) with the modified function projective synchronization, we further define a novel hybrid synchronization scheme as below:

Definition 2 (Polynomial-Function-Based Synchronization): The basic drive systems (1)-(3) and the response system (4) are said to be polynomial-function-based synchronization, if and only if

$$\lim_{t\to\infty} \| \sum_{l=1}^{N_1} A_l x^{<l>}(t) + \sum_{m=1}^{N_2} B_m y^{<m>}(t) + \sum_{j=1}^{N_3} C_j z^{<j>}(t) - \Lambda(t) w(t) \| = 0, \tag{7}$$

where $A_l = diag\{a_{l,1}, \cdots, a_{l,n}\}$, $B_m = diag\{b_{m,1}, \cdots, b_{m,n}\}$ and $C_j = diag\{c_{j,1}, , \cdots, c_{j,n}\}$ are three sets of coefficient matrices. $\Lambda(t) = diag\{\lambda_1(t), \cdots, \lambda_n(t)\}$ refers to a reversible function scaling matrix whose element $\lambda_i(t)$ is continuously differentiable nonzero function with bound.

For convenience, we introduce the following symbols

$$P_{N_1}(x) = \sum_{l=1}^{N_1} A_l x^{<l>}(t),$$

$$P_{N_2}(y) = \sum_{m=1}^{N_2} B_m y^{<m>}(t),$$

$$P_{N_3}(z) = \sum_{j=1}^{N_3} C_j z^{<j>}(t),$$

and

$$\bar{P}(x, y, z) = P_{N_1}(x) + P_{N_2}(y) + P_{N_3}(z),$$

then, (7) will be be reduced to

$$\lim_{t\to\infty} \| P_{N_1}(x) + P_{N_2}(y) + P_{N_3}(z) - \Lambda(t) w(t) \| = 0 \tag{8}$$

or

$$\lim_{t\to\infty} \| \bar{P}(x, y, z) - \Lambda(t) w(t) \| = 0. \tag{9}$$

If it is the case, $\bar{P}(x, y, z)$ is called the compound drive system.

Remark 1: In practice, the level of the communication security is dependent on the complexity level of the drive system. The drive system in the polynomial-function-based synchronization is composed of multiple subsystems through nonlinear operation, so it is more complex. As shown in Table 1, the proposed hybrid synchronization scheme covers most all of the existing synchronization schemes. When we choose specific scaling matrix $\Lambda(t)$ and the synchronization lags, the polynomial-function-based synchronization will be reduced to different specific ones. Here $\Lambda = diag\{\lambda_1, \cdots, \lambda_n\}$, and I refers to the $n \times n$ unit matrix.

As shown in Figs 1 and 2, compared with the three basic drive systems, the chaotic topology is more complicated. Moreover, by increasing the power of the polynomial function, the diameter of the chaotic manifold of the compound drive system becomes much longer, which means more types of signals can be transmitted.

Denote the following synchronization error

$$e(t) = \bar{P}(x, y, z) - \Lambda(t) w(t)$$

TABLE 1. Comparison of the proposed synchronization scheme with other existing ones.

	Parameter selection	Synchronous name	Synchronization error
		Polynomial-function-based synchronization	$e(t) = \sum_{l=1}^{N_1} A_l x^{<l>}(t) + \sum_{m=1}^{N_2} B_m y^{<m>}(t) + \sum_{j=1}^{N_3} C_j z^{<j>}(t) - \Lambda(t)w(t)$
Case 1	$N_1 = N_2 = 1, N_3 = 0, \Lambda(t) = \Lambda$	**Combination synchronization**	$e(t) = A_1 x(t) + B_1 y(t) - \Lambda w(t)$
Case 2	$N_1 = 1, N_2 = N_3 = 0, C_1 = I$	**Modified function projective synchronization**	$e(t) = x(t) - \Lambda(t)w(t)$
Case 3	$N_1 = 1, N_2 = N_3 = 0, A_1 = I, \Lambda(t) = \Lambda$	**Projective synchronization**	$e(t) = x(t) - \Lambda w(t)$
Case 4	$N_1 = 1, N_2 = N_3 = 0, A_1 = \Lambda(t) = I$	**Complete synchronization**	$e(t) = x(t) - w(t)$
Case 5	$N_1 = 1, N_2 = N_3 = 0, A_1 = -\Lambda(t) = I$	**Anti-synchronization**	$e(t) = x(t) + w(t)$

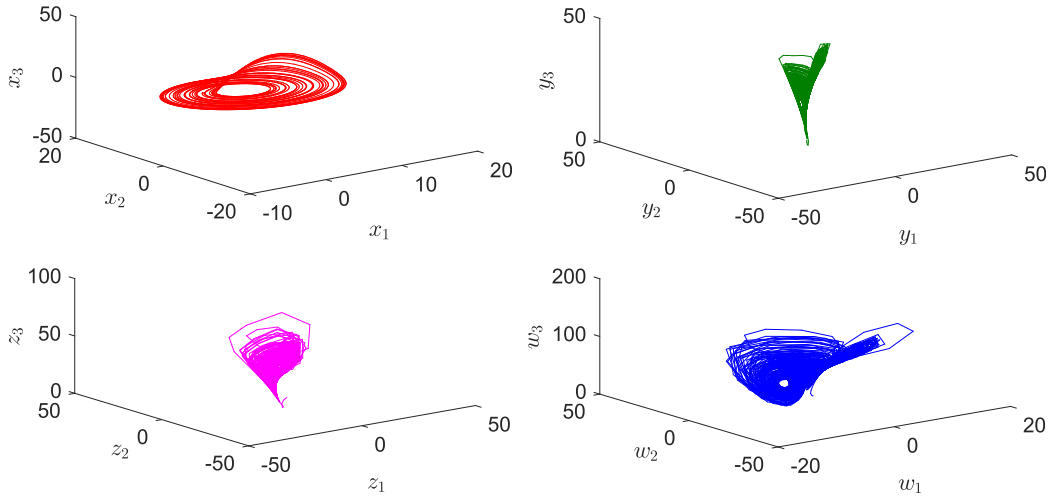

FIGURE 1. Phase portraits of the chaotic systems involved in this work.

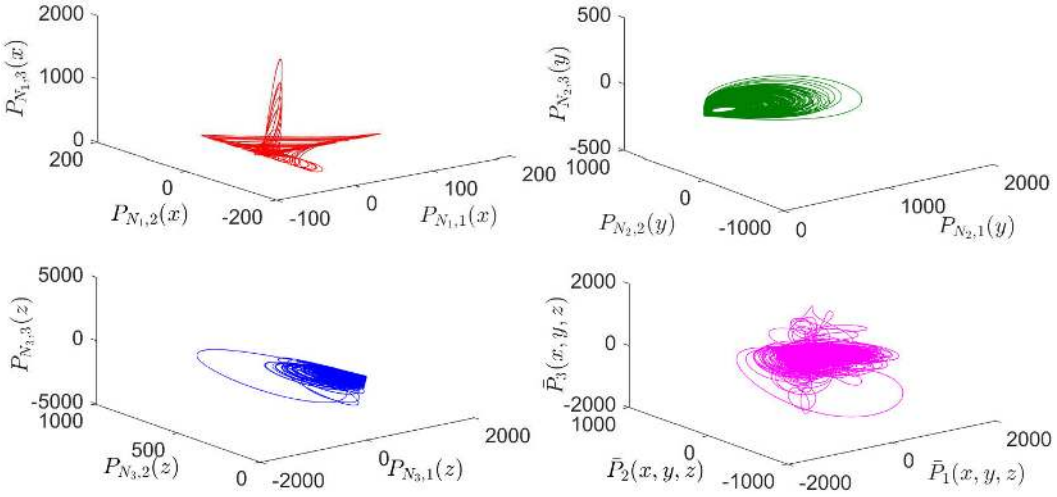

FIGURE 2. Phase portrait of the compound drive system based on polynomial-function.

or

$$\begin{aligned} e_i(t) &= \bar{P}_i(x, y, z) - \lambda_i(t)w(t) \\ &= \sum_{l=1}^{N_1} a_{l,i} {x_i}^l(t) + \sum_{m=1}^{N_2} b_{m,i} {y_i}^m(t) \\ &\quad + \sum_{j=1}^{N_3} c_{j,i} {z_i}^j(t) - \lambda_i(t)w_i(t) \\ i &= 1, 2, \cdots, n, \end{aligned}$$

then the error system among chaotic systems (1)-(4) can be obtained as below

$$\dot{e}_i(t) = \Omega_i - \lambda_i(t)u_i(t), \tag{10}$$

in which

$$\Omega_i = \sum_{l=1}^{N_1} l a_{l,i} x_i^{l-1}(t)(F_i(t)\theta + f_i(t))$$

TABLE 2. Comparison of the predefined-time stability with other well-known stabilities.

Stability name	Definition	Characteristic
Asymptotically stability	The origin of system (11) satisfies $\lim_{t\to\infty}\chi(t,\chi_0)=0$.	The stability time of the system is long and is not necessarily bounded.
Finite-time stability [16]	The origin of system (11) is globally asymptotically stable and there exists a finite time $T(\chi_0)\geq 0$, such that $\lim_{t\to T(\chi_0)-}\chi(t,\chi_0)=0$, and $\chi(t,\chi_0)\equiv 0, \forall t\geq T(\chi_0)$.	The stabilization time is limited, however, it depends on the initial state χ_0 and its' upper bound can not be determined.
Fixed-time stability [19]	The origin of system (11) is finite-time stable and the settling-time function $T(\chi_0)$ is bounded, i.e., there exists a constant $T_{max}\geq 0$ such that $T(\chi_0)\leq T_{max}, \forall\chi_0\in R^n$.	T_{max} is independent of the initial state, but it need to be estimated according to the control parameters.
Predifined-time stability in this work	The origin of system (11) is fixed-time stable and for an predefined settling time $T_p\geq 0$, it hold for any initial state χ_0 that $\lim_{t\to T_p-}\chi(t,\chi_0)=0$ and $\chi(t,\chi_0)\equiv 0, \forall t\geq T_p$.	T_p can be preassigned off-line according to the control task, so it is independent of the initial state χ_0 and other control parameters.

$$+\sum_{m=1}^{N_2} mb_{m,i}y_i^{m-1}(t)(G_i(y)\phi+g_i(y))$$
$$+\sum_{j=1}^{N_3} jc_{j,i}z_i^{j-1}(t)(H_i(z)\eta+h_i(z))$$
$$-\dot{\lambda}_i(t)w_i(t)-\lambda_i(t)(R_i(w)\varphi+r_i(w))$$

and $i=1,2,\cdots,n$.

B. PREDEFINED-TIME STABILITY AND PREDEFINED-TIME SYNCHRONIZATION

Consider the dynamical system

$$\dot{\chi}(t)=\varphi(t,\chi;\sigma),\quad t\in[0,+\infty) \tag{11}$$

where $\chi\in R^n$ stands for the system state, $\sigma\in R^m$ represents the system parameter. Assume the origin is an equilibrium point of the system (11) and denote $\chi_0=\chi(0)$, then $\varphi(0,\chi_0;\sigma)=0$.

Definition 3 (Predefined-Time Stability [23]): The origin of system (11) is said to be globally predefined-time stable, if for an appointed settling-time $T_p\geq 0$, the following equations hold for all initial state χ_0

$$\lim_{t\to T_p-}\chi(t,\chi_0)=0, \tag{12}$$

and

$$\chi(t,\chi_0)\equiv 0,\quad \forall t\geq T_p. \tag{13}$$

If this is the case, T_p is called a predefined-time.

Lemma 1: [18] For four positive constants γ_1, γ_2, ε_1 and ε_1, if there exists a continuous radially unbounded Lyapunov function $V: R^n\to R$ for the dynamics system (11) and it satisfies

$$\dot{V}=\vartheta(V), \tag{14}$$
$$\vartheta(V)\leq -(\gamma_1V^{\varepsilon_1}+\gamma_2V^{\varepsilon_2}), \tag{15}$$

Then,

1) if $\varepsilon_1,\varepsilon_2\in[0,1)$, then, the origin of system (11) is finite-time stable and the settling time is estimated as

$$T(\chi_0)\leq min\{\frac{V^{1-\varepsilon_1}(\chi_0)}{\gamma_1(1-\varepsilon_1)},\frac{V^{1-\varepsilon_2}(\chi_0)}{\gamma_2(1-\varepsilon_2)}\}; \tag{16}$$

2) if $\varepsilon_1\in(1,+\infty)$, $\varepsilon_2\in[0,1)$, then, the origin of system (11) is fixed-time stable and the settling time is estimated as

$$T_{max}\leq\frac{1}{\gamma_1(1-\varepsilon_1)}+\frac{1}{\gamma_2(1-\varepsilon_2)}. \tag{17}$$

Lemma 2: [24] For any preappointed constant $T_p>0$, if there exists a radially unbounded Lyapunov function $V: R^n\to R$ for the dynamics system (11) and it satisfies

$$\dot{V}=\vartheta(V), \tag{18}$$
$$\vartheta(V)\leq-\frac{\pi}{\alpha T_p}(V^{1+\frac{\alpha}{2}}+V^{1-\frac{\alpha}{2}}), \tag{19}$$

where $\alpha\in(0,1)$ is a real constant.

Then, the origin of system (11) is predefined-time stable within the predefined-time T_p.

Remark 2: Predefined-time stability is an upgrade of fixed-time stability, and

$$T_p=\sup T(\chi_0),\quad \forall\chi_0\in R^n. \tag{20}$$

It can be shown from the comparison of Table 2 that, the conservatism of the four kinds of stability decreases in turn, and the flexibility increases in turn. Form Lemma 1 one can see, for finite-time stability and fixed-time stability, it is difficult to find the explicate relationship between the system parameters and the settling time, which lead to overestimation of the convergence time. However, the settling time $T_p>0$ in predefined-time stability can be assigned in advance without estimation or conservatism, and it can be arbitrarily small, so it is very valuable in practical applications.

Definition 4 (Predefined-Time Polynomial-Function-Based Synchronization): The four chaotic systems (1)-(4) are said to be predefined-time polynomial-function-based synchronization if and only if the origin of the synchronization error system (10) is predefined-time stable within any preassigned time $T_p>0$.

III. DESIGN OF THE PREDEFINED-TIME SYNCHRONIZATION CONTROL SCHEME

The main task of this work is to design a synchronization control algorithm to achieve the predefined-time polynomial-function-based synchronization among the four chaotic systems (1)-(4). The control scheme will be realized by means of the terminal sliding mode control technology.

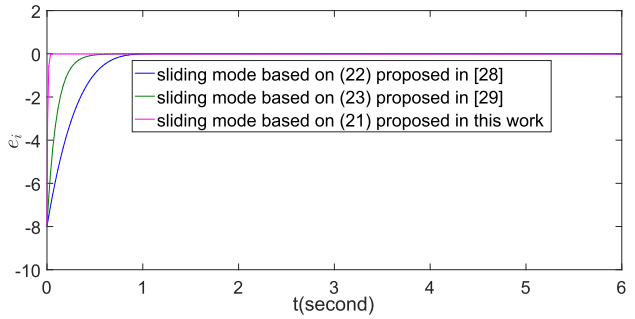

FIGURE 3. Comparison of three sliding modes.

A. SLIDING MODE PHASE

To ensure the predefined-time stable of the sliding mode, we propose a novel nonsingular integral terminal sliding mode function as below,

$$s_i(t) = e_i(t) + \int_0^t (c_1 e_i(\tau) + c_2 \text{sign}(e_i(\tau))|e_i(\tau)|^{1+\alpha_1} + c_3 \text{sign}(e_i(\tau))|e_i(\tau)|^{1-\alpha_1}) d\tau, \quad (21)$$

where $0 < \alpha_1 < 1$, $c_1 > 0$, $c_2 = \frac{\pi}{2^{1+\frac{\alpha_1}{2}} \alpha_1 T_{p,1}}$ and $c_3 = \frac{\pi}{2^{1-\frac{\alpha_1}{2}} \alpha_1 T_{p,1}}$ represent the sliding mode parameters, $i = 1, 2, \cdots, n$.

Remark 3: Compared with the following two traditional integral terminal sliding mode function proposed in [28] and [29]

$$s_i(t) = e_i(t) + c \int_0^t sign(e_i(\tau))|e_i(\tau)|^{\alpha} d\tau, \; c > 0, \quad 0 < \alpha < 1, \quad (22)$$

$$s_i(t) = e_i(t) + c \int_0^t e_i(\tau) d\tau, \; c > 0, \quad (23)$$

the sliding mode function (21) is multi-power, which ensure the error system to maintain a faster convergence rate throughout the sliding mode phase.

As shown in Fig.3, compared with (22) and (23), the sliding mode function (21) designed in this work can ensure the error system (10) converges to the equilibrium point $e_i(t) = 0$ faster during the sliding mode phase, and the convergence time can be pre-assigned, so it is more flexible. Here the error system is started from $e_i(0) = -8$ with $i = 1$, and the convergence time during the sliding mode phase based on (21) is predefined as $T_{p,1} = 0.1$.

Let

$$s_i(t) = \dot{s}_i(t) = 0, \quad i = 1, 2, \cdots, n,$$

then, the dynamics of sliding mode can be obtained as

$$\dot{e}_i(t) = -(c_1 e_i(t) + c_2 \text{sign}(e_i(t))|e_i(t)|^{1+\alpha_1} + c_3 \text{sign}(e_i(t))|e_i(t)|^{1-\alpha_1}), \quad i = 1, 2, \cdots, n. \quad (24)$$

Theorem 1: For any predefined-time $T_p > 0$, if we set $T_{p,1} = \beta_1 T_p$ with the weighted gain $\beta_1 \in (0, 1)$, then the sliding mode (24) will be predefined-time stable within the predefined-time $T_{p,1}$, i.e., the trajectory $e(t)$ on the sliding surface $s(t) = [s_1(t), s_2(t), \cdots, s_n(t)]^T = 0$ will converge to the equilibrium $e(t) = 0$ within $T_{p,1}$.

Proof: Select the Lyapunov function

$$V_{1,i}(t) = \frac{1}{2} e_i^2(t), \quad i = 1, 2, \cdots, n. \quad (25)$$

Take the derivative of $V_{1i}(t)$ along the sliding mode (24), we calculate

$$\begin{aligned} V_{1,i}(t) &= e_i(t)\dot{e}_i(t) \\ &= -c_1(e_i(t))^2 - c_2|e_i(t)|^{2+\alpha_1} - c_3|e_i(t)|^{2-\alpha_1} \\ &= -2c_1 V_{1,i} - \frac{\pi}{\alpha_1 T_{p,1}}((V_{1,i})^{1+\frac{\alpha_1}{2}} + (V_{1,i})^{1-\frac{\alpha_1}{2}}) \\ &\le -\frac{\pi}{\alpha_1 T_{p,1}}((V_{1,i})^{1+\frac{\alpha_1}{2}} + (V_{1,i})^{1-\frac{\alpha_1}{2}}). \end{aligned} \quad (26)$$

By mean of Lemma 2, we can derive that, each element $e_i(t)$ will converge to zero within the predefined time $T_{p,1}$ during the sliding mode phase, where $i = 1, 2, \cdots, n$. Thus the error vector $e(t)$ will converge to the origin within the predefined time $T_{p,1}$ along the sliding mode surface $s_(t) = 0$. □

B. SLIDING MODE APPROACHING PHASE

Notice the predefined-time stable sliding mode has been designed. Now we design the following sliding mode approaching controller to ensure the formation of the sliding mode in the predefined-time $T_{p,2}$,

$$\begin{aligned} u_i(t) &= \frac{1}{\lambda_i(t)}(c_1 e_i + c_2 \text{sign}(e_i)|e_i|^{1+\alpha_1} + c_3 \text{sign}(e_i)|e_i|^{1-\alpha_1} \\ &\quad + k_1 \text{sign}(s_i)|s_i|^{1+\alpha_2} + k_2 \text{sign}(s_i)|s_i|^{1-\alpha_2} + \Omega_i), \end{aligned} \quad (27)$$

where $k_1 = \frac{\pi}{2^{1+\frac{\alpha_2}{2}} \alpha_2 T_{p,2}}$, $k_2 = \frac{\pi}{2^{1-\frac{\alpha_2}{2}} \alpha_2 T_{p,2}}$ refer to the control gains, and $i = 1, 2, \cdots, n$.

Theorem 2: For the predefined-time T_p given in Theorem 1, if we set $T_{p,2} = \beta_2 T_p$ with the weighted gain $\beta_2 \in (0, 1)$ which satisfies $\beta_1 + \beta_2 = 1$, then the existence of the sliding mode (24) will be realized with in the predefined-time $T_{p,2}$ under the action of the control law (27).

Proof: Choose the Lyapunov function

$$V_{2,i}(t) = \frac{1}{2} s_i^2, \quad i = 1, 2, \cdots, n. \quad (28)$$

Then, the derivative of $V_{2,i}(t)$ is derived as

$$\begin{aligned} \dot{V}_{2,i}(t) &= s_i \dot{s}_i \\ &= s_i(\dot{e}_i(t) + (c_1 e_i(t) + c_2 \text{sign}(e_i(t))|e_i(t)|^{1+\alpha_1} \\ &\quad + c_3 \text{sign}(e_i(t))|e_i(t)|^{1-\alpha_1})) \\ &= -s_i(k_1 \text{sign}(s_i)|s_i|^{1+\alpha_2} + k_2 \text{sign}(s_i)|s_i|^{1-\alpha_2}) \end{aligned}$$

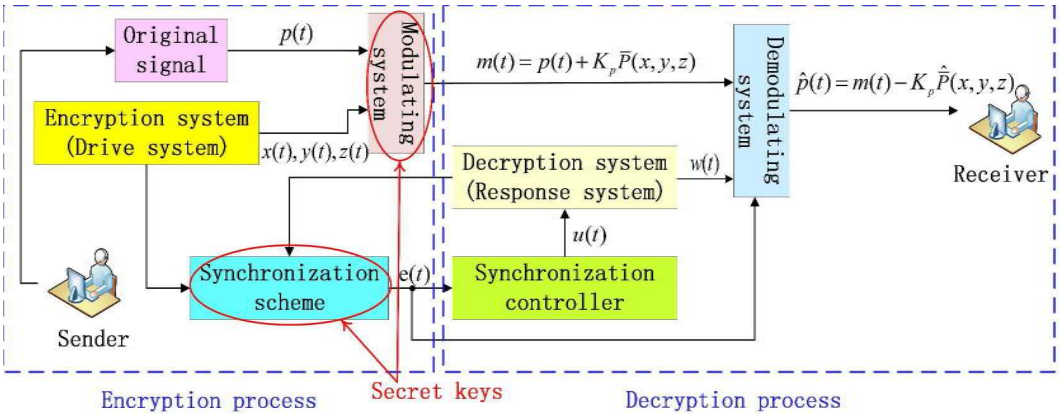

FIGURE 4. Framework of the proposed chaotic secure communication.

$$= -k_1 |s_i|^{2+\alpha_2} - k_2 |s_i|^{2-\alpha_2}$$
$$= -\frac{\pi}{\alpha_2 T_{p,2}}((V_{2,i})^{1+\frac{\alpha_2}{2}} + (V_{2,i})^{1-\frac{\alpha_2}{2}}). \quad (29)$$

Hence, it follows from Lemma 2 that each error trajectory $e_i(t)$ will reach the corresponding sliding surface $s_i(t) = 0$ in the predefined time $T_{p,2}$ and then remain on it forever. That is to say, the formation of the sliding mode will be realized with in the predefined-time$T_{p,2}$. □

Remark 4: Combining the results of Theorem 1 and Theorem 2, applying the control law (27), the predefined-time polynomial-function-based synchronization among the chaotic systems (1)-(4) will be realized within the appointed time $T_{p,1} + T_{p,2} = \beta_1 T_p + \beta_2 T_p = T_p$.

IV. SIMULATION EXPERIMENT

In this section, a simulation experiment of chaotic secure communication is present to illustrate the feasibility and effectiveness of the theoretical results.

The framework of chaotic secure communication is shown in Fig. 4 and the basic principle is explicated as below:

At the sender end, three chaotic signals $x(t)$, $y(t)$ and $z(t)$ are generated by the basic drive systems as the carrier signals, and then the original message $p(t)$ transmitted by the sender is modulated into the encrypted message as $m(t) = p(t) + K_p\bar{P}(x, y, z)$, which will be transmitted to the receiver through the message transmission channel. At the receiver end, the response system keeps in synchronization with the drive system according to a specific relationship applying the control algorithm $u(t)$ and reverses the compound carrier signal $\hat{\bar{P}}(x, y, z)$, then recover the message $\hat{p}(t) = m(t) - K_p\hat{\bar{P}}(x, y, z)$ based on the message modulation scheme.

In the process of chaotic secure communication, even if the attacker intercepts $m(t)$ and obtain $w(t)$, if he wants to obtain the encrypted signal $p(t)$, he must known the secret keys of message modulation scheme and chaotic synchronization scheme. Hence enhancing the complexity of modulation scheme and synchronization scheme are the main ways to improve the defense capability of secure communications.

According to Definition 4, the synchronization scheme applied in this secure communication experiment is designed as

$$\lim_{t\to T_p-} \|e(t)\| = \lim_{t\to T_p-} \left\|\bar{P}(x, y, z) - \Lambda(t)w(t)\right\| = 0,$$
$$\|e(t)\| = \left\|\bar{P}(x, y, z) - \Lambda(t)w(t)\right\| \equiv 0, \quad \text{if } t \geq T_p \quad (30)$$

in which $T_p > 0$ is the predefined synchronization time, $\bar{P}(x, y, z) = P_{N_1}(x) + P_{N_2}(y) + P_{N_3}(z)$, $N_1 = 3$, $N_2 = 2$, $N_3 = 3$, and the coefficient matrix of the polynomial function are taken as

$$A_1 = diag\{1, -2, 2\},$$
$$A_2 = diag\{1, 1, 0.5\},$$
$$A_3 = diag\{-0.1, 0.2, 0.1\},$$
$$B_1 = diag\{1, 2, -3\},$$
$$B_2 = diag\{2, -1, 0.2\},$$

and

$$C_1 = diag\{3, -1, 0.5\},$$
$$C_2 = diag\{-1, 0.5, 0\},$$
$$C_2 = diag\{0.01, 0, -0.01\}.$$

Meanwhile, the synchronization scaling matrix is given as

$$\Lambda(t) = diag\{(1-0.5\sin t)^{-1}, (2-0.2\cos 2t)^{-1}, (-2-\sin t)^{-1}\}.$$

Three famous chaotic systems Rössler system, Lü system and Chen system are adopted as the basic drive systems while another famous chaotic system Liu system is applied as the response system, the mathematical models of the above four systems are described as:

Rössler system

$$\begin{pmatrix}\dot{x}_1\\ \dot{x}_2\\ \dot{x}_3\end{pmatrix} = \underbrace{\begin{pmatrix}-x_2 - x_3 & 0 & 0\\ x_1 & x_2 & 0\\ 0 & 0 & -x_3\end{pmatrix}}_{F(x(t))}\underbrace{\begin{pmatrix}1\\ 0.2\\ 5.7\end{pmatrix}}_{\theta} + \underbrace{\begin{pmatrix}0\\ 0\\ x_1x_3 + 0.2\end{pmatrix}}_{f(x(t))}, \quad (31)$$

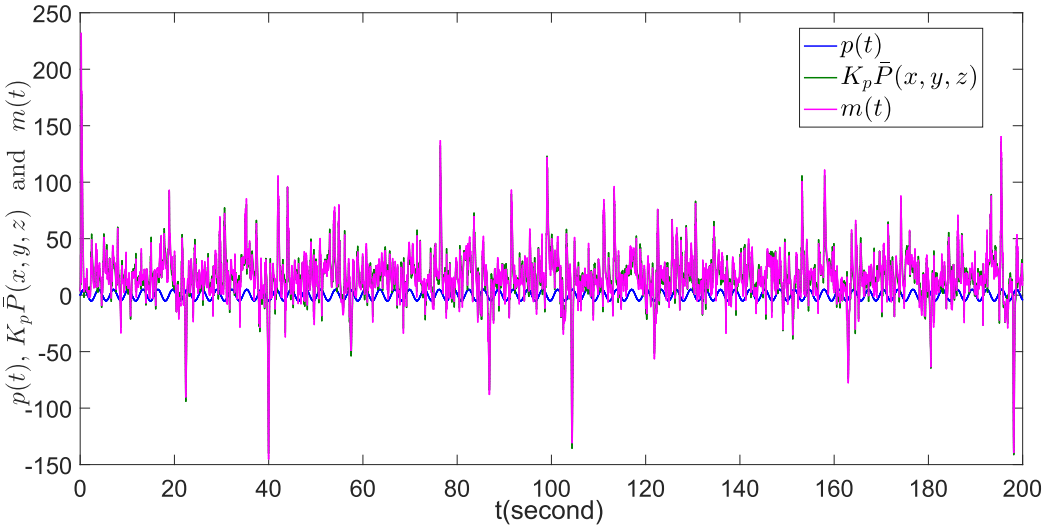

FIGURE 5. Comparison among original message $p(t)$, carrier signal $K_p\bar{P}(x, y, z)$ and encrypted message $m(t)$.

Lü system

$$\begin{pmatrix}\dot{y}_1\\ \dot{y}_2\\ \dot{y}_3\end{pmatrix} = \underbrace{\begin{pmatrix}y_2-y_1 & 0 & 0\\ 0 & y_2 & 0\\ 0 & 0 & -y_3\end{pmatrix}}_{G(y(t))}\underbrace{\begin{pmatrix}36\\ 20\\ 3\end{pmatrix}}_{\phi} + \underbrace{\begin{pmatrix}0\\ -y_1y_3\\ y_1y_2\end{pmatrix}}_{g(y(t))}, \quad (32)$$

Chen system

$$\begin{pmatrix}\dot{z}_1\\ \dot{z}_2\\ \dot{z}_3\end{pmatrix} = \underbrace{\begin{pmatrix}z_2-z_1 & 0 & 0\\ -z_1 & z_1+z_2 & 0\\ 0 & 0 & -z_3\end{pmatrix}}_{H(z(t))}\underbrace{\begin{pmatrix}35\\ 28\\ 3\end{pmatrix}}_{\eta} + \underbrace{\begin{pmatrix}0\\ -z_1z_3\\ z_1z_2\end{pmatrix}}_{h(z(t))}, \quad (33)$$

Liu system

$$\begin{pmatrix}\dot{w}_1\\ \dot{w}_2\\ \dot{w}_3\end{pmatrix} = \underbrace{\begin{pmatrix}w_2-w_1 & 0 & 0\\ 0 & w_1 & 0\\ 0 & 0 & -w_3\end{pmatrix}}_{R(w(t))}\underbrace{\begin{pmatrix}10\\ 40\\ 2.5\end{pmatrix}}_{\psi} + \underbrace{\begin{pmatrix}0\\ -w_1w_3\\ 4(w_1)^2\end{pmatrix}}_{r(w(t))} + \underbrace{\begin{pmatrix}u_1(t)\\ u_2(t)\\ u_3(t)\end{pmatrix}}_{u(t)}, \quad (34)$$

with the initial states $x(0) = (-3, 3, -2)^T$, $y(0) = (-1, -2, 4)^T$, $z(0) = (3, -3, 2)^T$ and $w(0) = (2, 2, 2)^T$.

The comparison of Figs.1-2 indicates that the compound drive system based on polynomial-function is more complex without loss of the chaotic characteristic. When it is adopted as the carrier signal, it can effectively enhance the concealment of message.

The original message in this secure communication is chosen as

$$p(t) = 5\sin 2t,$$

and the modulation scheme is designed as

$$\begin{aligned} m(t) &= p(t) + K_p\bar{P}(x, y, z)\\ &= p(t) + 0.1\bar{P}_1(x, y, z) + 0.2\bar{P}_2(x, y, z)\\ &\quad - 0.1\bar{P}_3(x, y, z). \end{aligned} \quad (35)$$

As shown in Fig.5, based on the modulation scheme (35), the bandwidth of the original message $p(t)$ is far less than that of the carrier signal $K_p\bar{P}(x, y, z)$, and the encrypted message $m(t)$ is more complex and more difficult to predict than $p(t)$, which means the modulated scheme has good anti-aggression.

According to Theorems 1-2, we carry out the simulation based on the predefined-time sliding mode control algorithm (21) and (27). The parameters in the sliding mode function are given as $\alpha_1 = 0.25$, $\alpha_2 = 0.2$, $c_{i1} = 200$, the predefined synchronization time is assigned as $T_p = 1$ and the weighted gains are distributed as $\beta_1 = 0.8$, $\beta_2 = 0.2$. Accordingly, the parameters related to T_p is calculated by

$$\begin{aligned} c_{i2} &= \frac{\pi}{2^{1+\frac{\alpha_1}{2}}\alpha_1\beta_1\, T_p},\\ c_{i3} &= \frac{\pi}{2^{1-\frac{\alpha_1}{2}}\alpha_1\beta_1 T_p},\\ k_1 &= \frac{\pi}{2^{1+\frac{\alpha_2}{2}}\alpha_2\beta_2\, T_p},\\ k_2 &= \frac{\pi}{2^{1-\frac{\alpha_2}{2}}\alpha_2\beta_2\, T_p}. \end{aligned}$$

Then, the simulation results are shown by Figs.6-Figs.9.

As shown in Figs.6-7, even if the predefined time T_p is assigned to be very short, the proposed synchronization scheme can guarantee the sliding mode is realized within the predefined time $\beta_2\, T_p = 0.2$ and the synchronization error $e_i(t)$ converges to zero within the predefined time

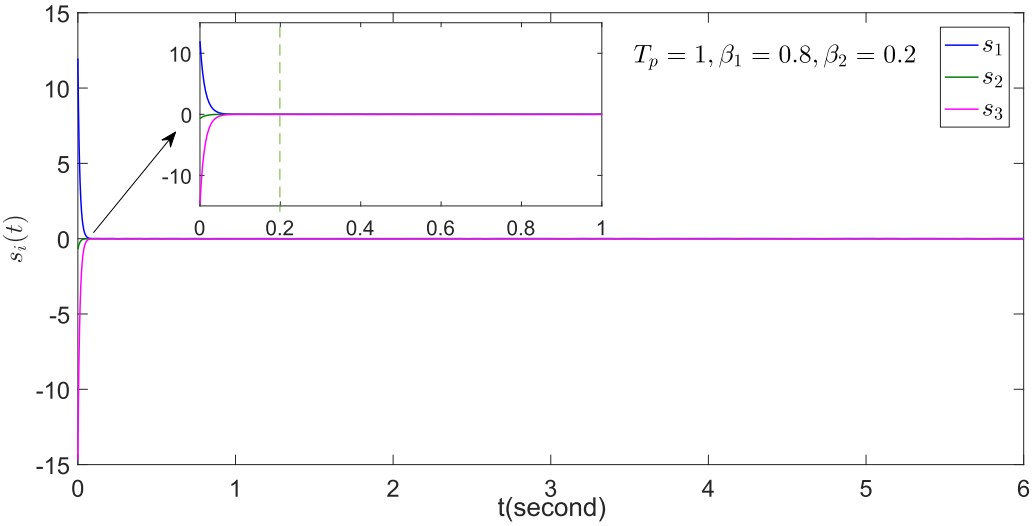

FIGURE 6. Time response of sliding mode surface function $s(t)$ with $T_p = 1$, $\beta_1 = 0.8$, $\beta_2 = 0.2$.

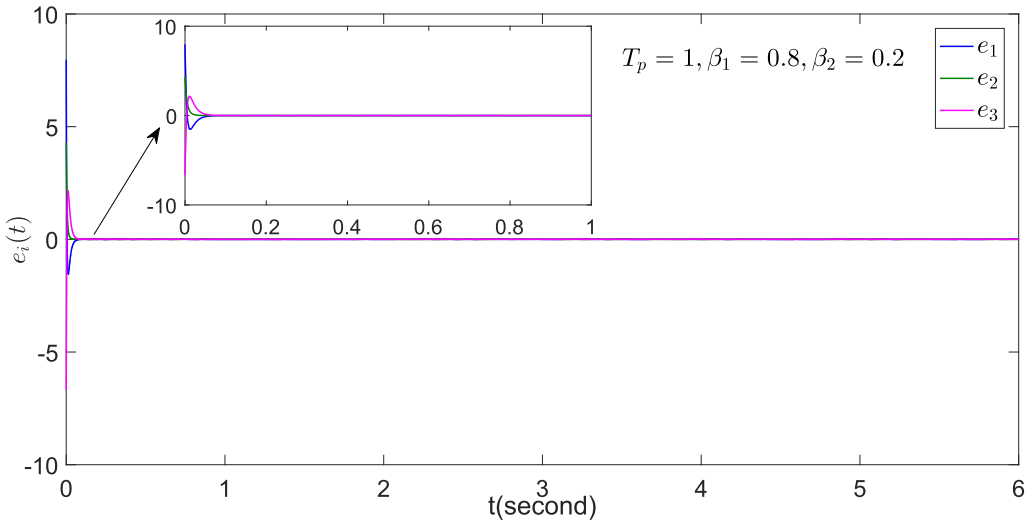

FIGURE 7. Time response of synchronization error e with $T_p = 1$, $\beta_1 = 0.8$, $\beta_2 = 0.2$.

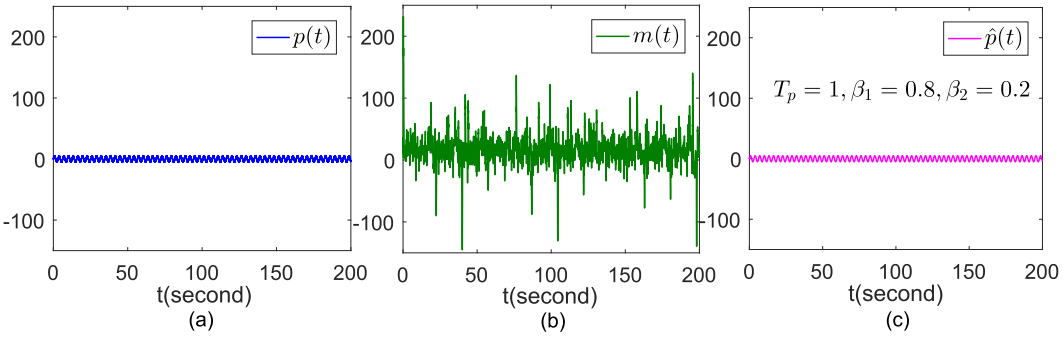

FIGURE 8. Comparison among the original, encrypted and decrypted messages with $T_p = 1$, $\beta_1 = 0.8$, $\beta_2 = 0.2$. (a) Original message $p(t)$. (b) Encrypted message $m(t)$. (c) Decrypted message $\hat{p}(t)$.

$T_p = 1$, which means the predefined-time polynomial-function-based polynomial-function among the multiple chaotic systems (31)-(34) is achieved successfully.

As shown in Fig.4, during the decryption process, the original message is decrypted using the secret keys of synchronization scheme (30) and the modulation scheme (35) by the

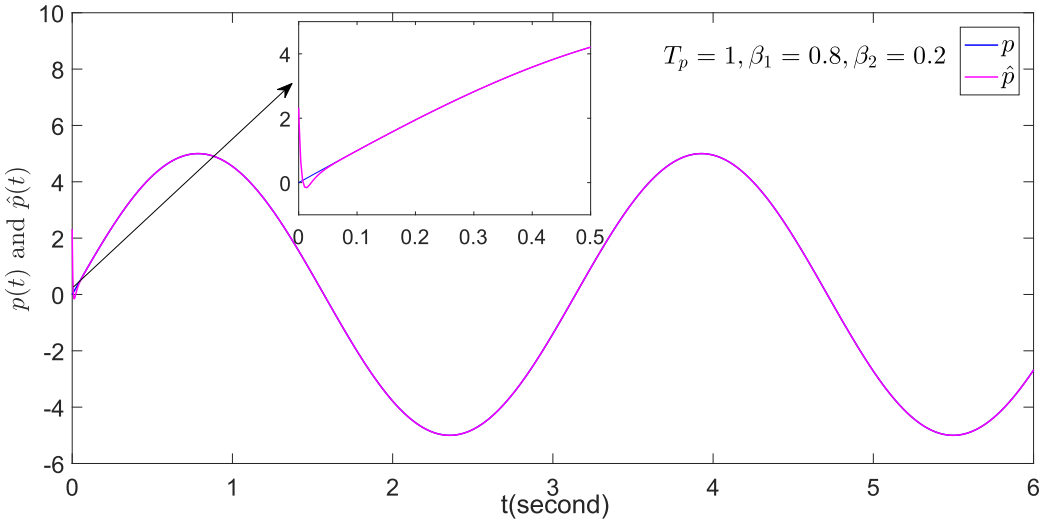

FIGURE 9. State trajectories of original message signal $p(t)$ and decrypted message $\hat{p}(t)$ with $T_p = 1, \beta_1 = 0.8, \beta_2 = 0.2$.

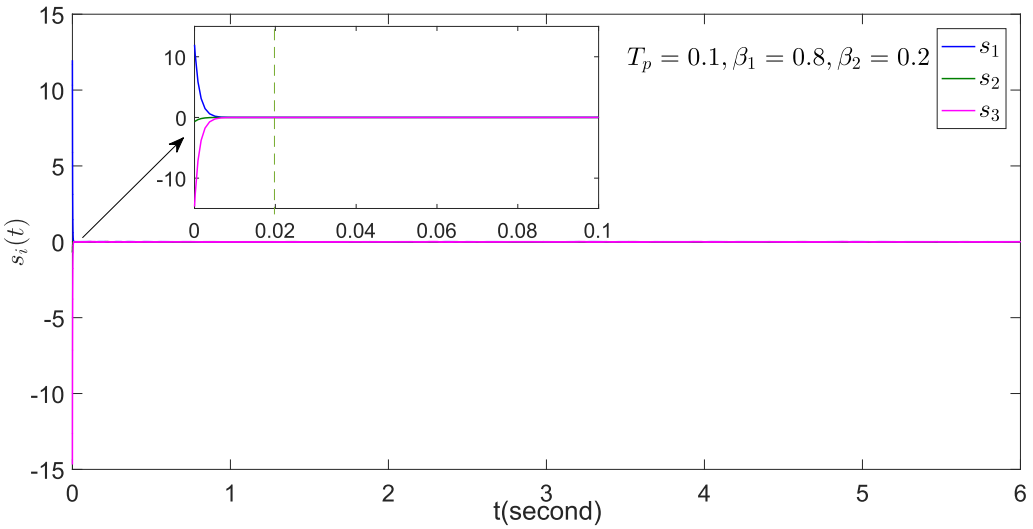

FIGURE 10. Time response of sliding mode surface function $s(t)$ with $T_p = 0.1, \beta_1 = 0.8, \beta_2 = 0.2$.

receiver.

$$\begin{aligned}\hat{p}(t) &= m(t) - K_p\hat{\bar{P}}(x, y, z)\\ &= m(t) - K_p\Lambda(t)w(t)\\ &= m(t) - (0.1\lambda_1(t)w_1(t) + 0.2\lambda_2(t)w_2(t)\\ &\quad - 0.1\lambda_3(t)w_3(t)).\end{aligned}$$

From Figs.8-9 one can see, the original message $p(t)$ is accurately recovered as $\hat{p}(t)$ within the predefined-time $T_p = 1$, which indicates the effectiveness of the proposed secure communication scheme.

Next, we cut down the predefined synchronization time to $T_p = 0.1$. From the simulation results depicted in Figs.10-13, one can see that the proposed synchronization control algorithm still ensures the encoded message is accurately recovered within the predefined time $T_p = 0.1$, so as to achieve high quality secure communication.

To further verify the advancement of the proposed synchronization control algorithm, we compare it with the well-known fixed-time synchronization control algorithm which is designed as

$$\begin{aligned}u_i(t) = \frac{1}{\lambda_i(t)}(\gamma_0\text{sign}(e_i) + (\frac{1}{2})^{\varepsilon_1}\gamma_1\text{sign}(e_i)|e_i|^{2\varepsilon_1-1}\\ + (\frac{1}{2})^{\varepsilon_1}\gamma_2\text{sign}(e_i)|e_i|^{2\varepsilon_2-1} + \Omega_i),\end{aligned} \quad (36)$$

where $\varepsilon_1 = 1.1$, $\varepsilon_2 = 0.9$, $\gamma_0 = 6$, $\gamma_1 = 5 \cdot 2^{\varepsilon_1}$, $\gamma_2 = 6 \cdot 2^{\varepsilon_2}$ and $i = 1, 2, \cdots, n$.

Choose the Lyapunov function

$$V_i(t) = \frac{1}{2}{e_i}^2(t), \quad i = 1, 2, \cdots, n,$$

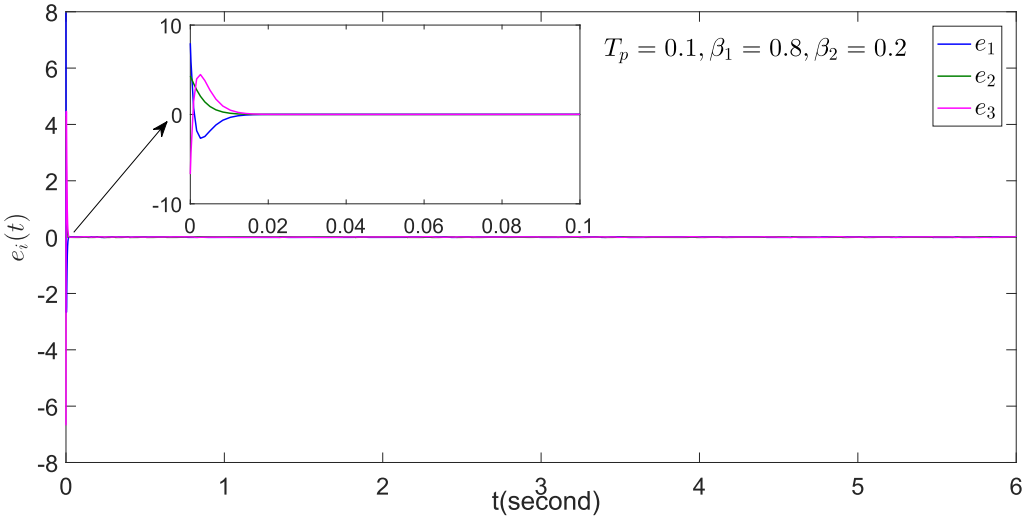

FIGURE 11. Time response of synchronization error $e(t)$ with $T_p = 0.1$, $\beta_1 = 0.8$, $\beta_2 = 0.2$.

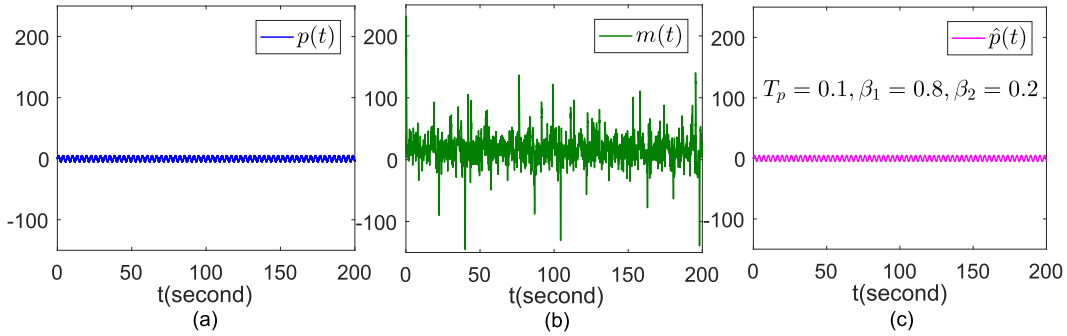

FIGURE 12. Comparison among the original, encrypted and decrypted messages with $T_p = 0.1$, $\beta_1 = 0.8$, $\beta_2 = 0.2$. (a) Original message $p(t)$. (b) Encrypted message $m(t)$. (c) Decrypted message $\hat{p}(t)$.

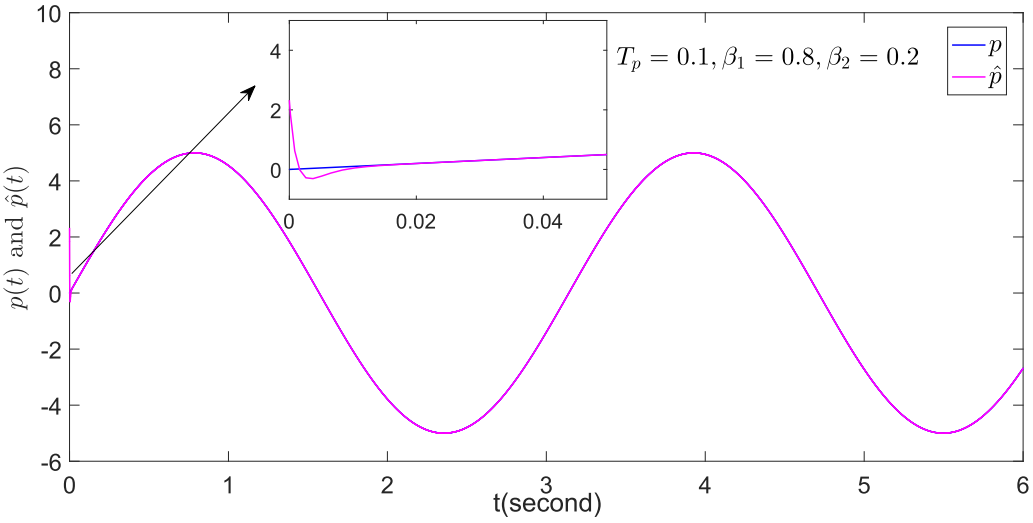

FIGURE 13. State trajectories of original message $p(t)$ and decrypted message $\hat{p}(t)$ with $T_p = 0.1$, $\beta_1 = 0.8$, $\beta_2 = 0.2$.

then, it is easy to derive

$$\dot{V}_i \leq -(\gamma_1 (V_i)^{\varepsilon_1} + \gamma_2 (V_i)^{\varepsilon_2}).$$

In view of Lemma 1, the fixed-time synchronization among (31)-(34) is achieved. The corresponding simulation results are displayed by Figs.14-16, from which one can see, although the above method can realize the secure communication, its' synchronization accuracy and synchronization rate are obviously inferior to the predefined-time synchronization scheme.

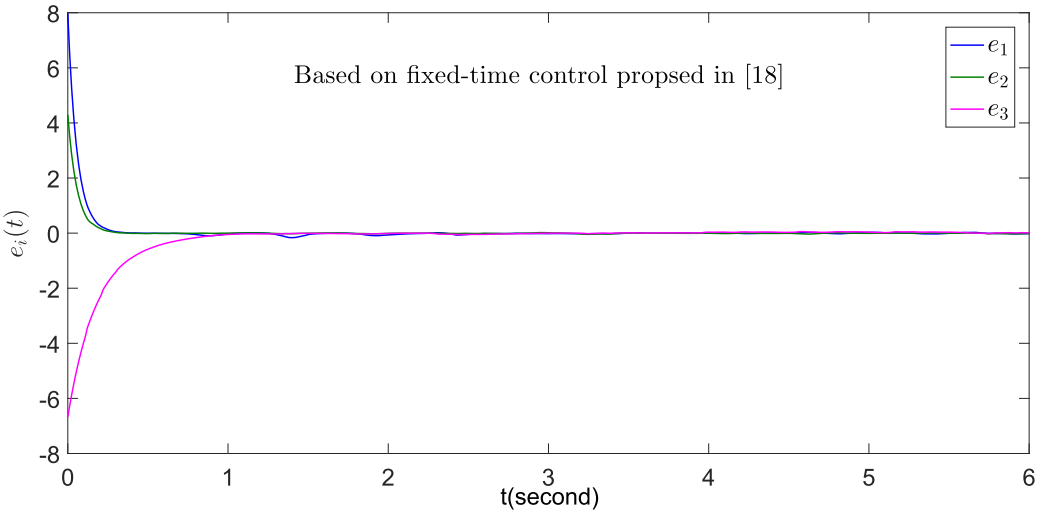

FIGURE 14. Time response of synchronization error $e(t)$ based on fixed-time control technique.

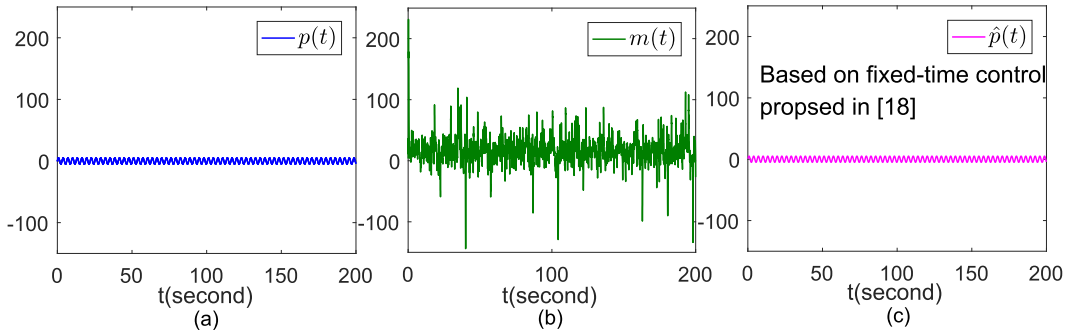

FIGURE 15. Comparison among the original, encrypted and decrypted messages based on fixed-time control technique. (a) Original message $p(t)$. (b) Encrypted message $m(t)$. (c) Decrypted message $\hat{p}(t)$.

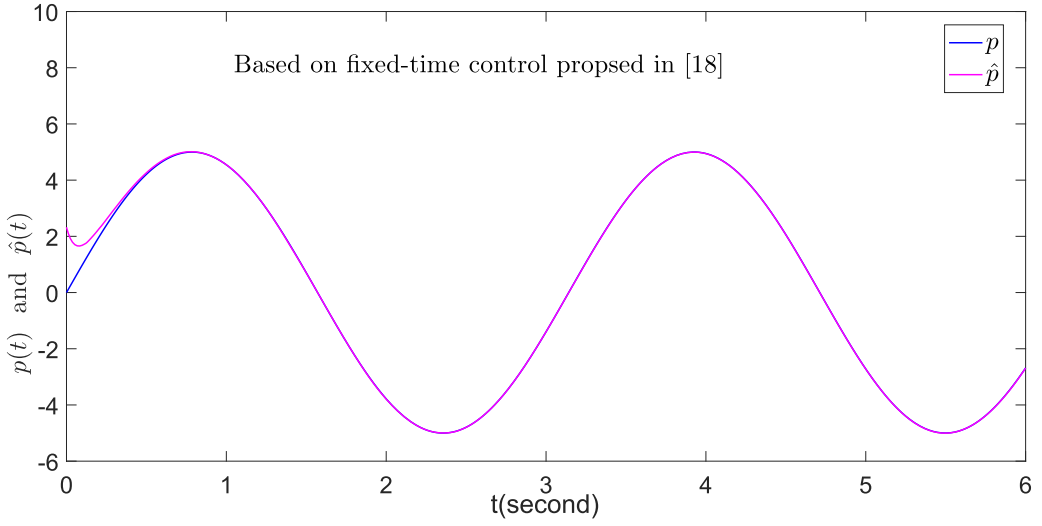

FIGURE 16. State trajectories of original message $p(t)$ and decrypted message $\hat{p}(t)$ based on fixed-time control technique.

V. CONCLUSION

In this article, the predefined-time polynomial-function-based synchronization of multiple chaotic systems has been investigated and applied in the chaotic secure communication. Theoretical results and simulation experiments show that, the novel polynomial-function-based

synchronization scheme can effectively improve the anti-decoding ability of secure communication, and the predefined-time synchronization algorithm based on the novel multi-power integral sliding mode control technology can effectively improve the decoding speed of the secure communication.

VI. FUTURE RECOMMENDATION

Firstly, the sliding mode control technique designed in this work is robust to the external noise. However, for the stronger noise, it is a better option to design a filter, a noise observer or an adaptive controller for the proposed synchronization control scheme, thus we will study it in detail as a follow-up work. Secondly, as known to all, synchronization of fractional chaotic systems is a generalization of synchronization of integer chaotic systems [30], so another subsequent work is applying the polynomial-function-based synchronization scheme to deal with the fractional-order chaotic synchronization problem. In addition, the consensus of multi-agent systems can be regarded as a generalization of synchronization problem [31], therefore, the study on the predefined-time consensus of multi-agent systems via the terminal sliding mode control technique designed in this work, is also valuable and challenging.

REFERENCES

[1] X. Chai, J. Zhang, Z. Gan, and Y. Zhang, "Medical image encryption algorithm based on Latin square and memristive chaotic system," *Multimedia Tools Appl.*, vol. 78, no. 24, pp. 35419–35453, Dec. 2019.

[2] J.-J. He and B.-C. Lai, "A novel 4D chaotic system with multistability: Dynamical analysis, circuit implementation, control design," *Mod. Phys. Lett. B*, vol. 33, no. 21, Jul. 2019, Art. no. 1950240.

[3] S. Mobayen and F. Tchier, "Synchronization of a class of uncertain chaotic systems with Lipschitz nonlinearities using state-feedback control design: A matrix inequality approach," *Asian J. Control*, vol. 20, no. 1, pp. 71–85, Jan. 2018.

[4] S. Zhang, Y. Zeng, Z. Li, M. Wang, and L. Xiong, "Generating one to four-wing hidden attractors in a novel 4D no-equilibrium chaotic system with extreme multistability," *Chaos, Interdiscipl. J. Nonlinear Sci.*, vol. 28, no. 1, Jan. 2018, Art. no. 013113.

[5] Q. Li and S. Liu, "Switching event-triggered network-synchronization for chaotic systems with different dimensions," *Neurocomputing*, vol. 311, no. 1, pp. 32–40, Oct. 2018.

[6] S. Mobayen and J. Ma, "Robust finite-time composite nonlinear feedback control for synchronization of uncertain chaotic systems with nonlinearity and time-delay," *Chaos, Solitons Fractals*, vol. 114, pp. 46–54, Sep. 2018.

[7] S. Mobayen, S. Vaidyanathan, A. Sambas, S. Kaçar, and Ü. Çavu oğlu, "A novel chaotic system with boomerang-shaped equilibrium, its circuit implementation and application to sound encryption," *Iranian J. Sci. Technol., Trans. Electr. Eng.*, vol. 43, no. 1, pp. 1–12, Mar. 2019.

[8] U. E. Kocamaz, S. Çiçek, and Y. Uyaroğlu, "Secure communication with chaos and electronic circuit design using passivity-based synchronization," *J. Circuits, Syst. Comput.*, vol. 27, no. 04, Apr. 2018, Art. no. 1850057.

[9] C. Nwachioma, J. H. Perez-Cruz, A. Jimenez, M. Ezuma, and R. Rivera-Blas, "A new chaotic oscillator—Properties, analog implementation, and secure communication application," *IEEE Access*, vol. 7, pp. 7510–7521, 2019.

[10] L. Runzi and W. Yinglan, "Finite-time stochastic combination synchronization of three different chaotic systems and its application in secure communication," *Chaos, Interdiscipl. J. Nonlinear Sci.*, vol. 22, no. 2, Jun. 2012, Art. no. 023109.

[11] Q. Li and S. Liu, "Dual-stage adaptive finite-time modified function projective multi-lag combined synchronization for multiple uncertain chaotic systems," *Open Math.*, vol. 15, no. 1, pp. 1035–1047, Aug. 2017.

[12] Q. Li, S. Liu, and Y. Chen, "Finite–Time adaptive modified function projective multi–lag generalized compound synchronization for multiple uncertain chaotic systems," *Int. J. Appl. Math. Comput. Sci.*, vol. 28, no. 4, pp. 613–624, Dec. 2018.

[13] A. J. Muñoz-Vázquez, J. D. S. Torres, and C. A. A. Gijón, "Single-channel predefined-time synchronisation of chaotic systems," *Asian J. Control*, vol. 1, no. 2, pp. 1–9, Aug. 2019.

[14] X. Liu, H. Su, and M. Z. Q. Chen, "A switching approach to designing finite-time synchronization controllers of coupled neural networks," *IEEE Trans. Neural Netw. Learn. Syst.*, vol. 27, no. 2, pp. 471–482, Feb. 2016.

[15] Y. Li, X. Yang, and L. Shi, "Finite-time synchronization for competitive neural networks with mixed delays and non-identical perturbations," *Neurocomputing*, vol. 185, no. 10, pp. 242–253, Apr. 2016.

[16] S. P. Bhat and D. S. Bernstein, "Finite-time stability of continuous autonomous systems," *SIAM J. Control Optim.*, vol. 38, no. 3, pp. 751–766, Jan. 2000.

[17] A. Levant and X. Yu, "Sliding-Mode-Based differentiation and filtering," *IEEE Trans. Autom. Control*, vol. 63, no. 9, pp. 3061–3067, Sep. 2018.

[18] X. Liu, D. W. C. Ho, Q. Song, and J. Cao, "Finite-/fixed-time robust stabilization of switched discontinuous systems with disturbances," *Nonlinear Dyn.*, vol. 90, no. 3, pp. 2057–2068, Nov. 2017.

[19] A. Polyakov, "Nonlinear feedback design for fixed-time stabilization of linear control systems," *IEEE Trans. Autom. Control*, vol. 57, no. 8, pp. 2106–2110, Aug. 2012.

[20] X. Yang, J. Lam, D. W. C. Ho, and Z. Feng, "Fixed-time synchronization of complex networks with impulsive effects via nonchattering control," *IEEE Trans. Autom. Control*, vol. 62, no. 11, pp. 5511–5521, Nov. 2017.

[21] G. Ji, C. Hu, J. Yu, and H. Jiang, "Finite-time and fixed-time synchronization of discontinuous complex networks: A unified control framework design," *J. Franklin Inst.*, vol. 355, no. 11, pp. 4665–4685, Jul. 2018.

[22] E. Jiménez-Rodríguez, J. D. Sânchez-Torres, and A. G. Loukianov, "On optimal predefined-time stabilization," in *Proc. 17th Latin Amer. Conf. Autom. Control*, Medellín, Colombia, Oct. 2016, pp. 317–322.

[23] J. D. Sánchez-Torres, D. Gómez-Gutiérrez, E. López, and A. G. Loukianov, "A class of predefined-time stable dynamical systems," *IMA Int. J. Robust Nonlinear Control*, vol. 35, no. 1, pp. 1–23, 2018.

[24] C. A. Anguiano-Gijón, A. J. Muñoz-Vázquez, J. D. Sánchez-Torres, G. Romero-Galván, and F. Martínez-Reyes, "On predefined-time synchronisation of chaotic systems," *Chaos, Solitons Fractals*, vol. 122, pp. 172–178, May 2019.

[25] C. R. Bheesayagari, J. Pons-Nin, M. T. Atienza, and M. Dominguez-Pumar, "Diffusive representation and sliding mode control of charge trapping in Al_2O_3 MOS capacitors," *IEEE Trans. Ind. Electron.*, vol. 66, no. 11, pp. 8628–8637, Nov. 2019.

[26] H. Du, X. Chen, G. Wen, X. Yu, and J. Lü, "Discrete-time fast terminal sliding mode control for permanent magnet linear motor," *IEEE Trans. Ind. Electron.*, vol. 65, no. 12, pp. 9916–9927, Dec. 2018.

[27] C.-S. Chiu, "Derivative and integral terminal sliding mode control for a class of MIMO nonlinear systems," *Automatica*, vol. 48, no. 2, pp. 316–326, Feb. 2012.

[28] M. P. Aghababa, S. Khanmohammadi, and G. Alizadeh, "Finite-time synchronization of two different chaotic systems with unknown parameters via sliding mode technique," *Appl. Math. Model.*, vol. 35, no. 6, pp. 3080–3091, Jun. 2011.

[29] M. Hou and Y. Wang, "A model-free adaptive integral terminal sliding mode control method," *Control Decis.*, vol. 33, no. 9, pp. 1591–1597, 2018.

[30] O. Mofid and S. Mobayen, "Adaptive synchronization of fractional-order quadratic chaotic flows with nonhyperbolic equilibrium," *J. Vib. Control*, vol. 78, pp. 35419–35453, Nov. 2017.

[31] H. Zhang, D. Yue, W. Zhao, S. Hu, and C. Dou, "Distributed optimal consensus control for multiagent systems with input delay," *IEEE Trans. Cybern.*, vol. 48, no. 6, pp. 1747–1759, Jun. 2018.

QIAOPING LI received the M.S. degree from the College of Mathematics and Information, Henan Normal University, Xinxiang, China, in 2007, and the Ph.D. degree from the School of Mathematics and Statistics, Xidian University, Xi'an, China, in 2019. Her research interests include synchronization of chaotic systems, network control systems, consensus of multi-agent systems, and sliding mode control.

CHAO YUE received the M.S. degree from the College of Science, Henan University of Science and Technology, Luoyang, China, in 2005, and the Ph.D. degree from the School of Mathematics and Statistics, Huazhong University of Science and Technology, Wuhan, China, in 2015. His research interest is numerical solution of differential equations.